



ELSEVIER

Available online at www.sciencedirect.com

ScienceDirect

journal homepage: www.elsevier.com/locate/he

Environmental and cost assessments criteria for selection of promising palladium membranes fabrication strategies

D. Alique ^{a,*}, P. Leo ^b, D. Martinez-Diaz ^c, J.A. Calles ^a, R. Sanz ^b

^a Department of Chemical, Energy and Mechanical Technology, Rey Juan Carlos University, Móstoles, Spain

^b Department of Chemical and Environmental Technology, Rey Juan Carlos University, Móstoles, Spain

^c Department of Applied Mathematics, Science and Engineering of Materials and Electronic Technology. Rey Juan Carlos University, Móstoles, Spain

HIGHLIGHTS

- Environmental impacts and costs for diverse Electroless Pore-Plating membranes.
- Porous CeO₂ improves membrane performance and cost but not the environmental impacts.
- Dense Pd–CeO₂ improves membrane performance, cost, and environmental impacts.
- Reduction of environmental impacts if scaling-up membrane length up to 25 cm.

ARTICLE INFO

Article history:

Received 24 January 2023

Received in revised form

12 March 2023

Accepted 25 April 2023

Available online xxx

Keywords:

Sustainable production

Life cycle assessment

Environmental impact

Cost analysis

Scale-up

Palladium membrane

ABSTRACT

Different strategies to prepare H₂-selective composite-membranes demonstrate promising performances, although the selection of the optimum alternative must consider environmental and economic concerns. These aspects, scarce in the available literature, are addressed here to analyze the convenience of using diverse CeO₂-based intermediate layers in composite Pd-membranes and recommend a maximum membrane length for scaling-up. The replacement of raw dense-CeO₂ by porous or Pd-doped particles in the intermediate layer clearly improves the membrane performance, saving around 50% of required Pd-thickness while increasing the H₂-permeance. However, porous-CeO₂ almost doubles the major environmental impacts and support modification costs, overcoming the potential saving costs in palladium. On the contrary, dense Pd-doped CeO₂ mitigates the environmental impacts by 27% and simultaneously saves 24% of expenses. Further reductions in environmental impacts and costs were reached after increasing the membrane-length up to 25 cm, becoming further improvements almost negligible for longer membranes.

© 2023 The Author(s). Published by Elsevier Ltd on behalf of Hydrogen Energy Publications LLC. This is an open access article under the CC BY-NC-ND license (<http://creativecommons.org/licenses/by-nc-nd/4.0/>).

* Corresponding author.

E-mail address: david.aliq@urjc.es (D. Alique).

<https://doi.org/10.1016/j.ijhydene.2023.04.292>

0360-3199/© 2023 The Author(s). Published by Elsevier Ltd on behalf of Hydrogen Energy Publications LLC. This is an open access article under the CC BY-NC-ND license (<http://creativecommons.org/licenses/by-nc-nd/4.0/>).

Introduction

Most industrial processes require certain separation steps to reach a concrete purity level to commercialize their final products. These steps are typically one of the largest energy-consuming operations in the industrial sector for many developed countries. This fact can be clearly illustrated by analyzing the total energy demand of the United States of America, taken as a model of a leading industrialized country, in which industrial processes represent up to a 35% of the total energy consumption, reaching around $25.9 \cdot 10^{15}$ Btu [1]. Particularly, chemical industries account for about 30% of the total energy demand of manufacturing sector, being the processes based on chemical separations responsible of around half of this consumption [2]. Considering that the energy system is still mainly based on fossil fuels and the imperative necessity of reducing the associated CO₂ emissions [3,4], the advances in new alternative and efficient separation technologies expect to help in the reduction of global environmental impacts coming from the industry. Among diverse possibilities, the development and use of highly selective membranes are attracting great attention for a wide variety of industrial applications such as wastewater treatment or gas purification [5–8]. Particularly, this trend can also relate to the promotion of hydrogen as a clean energy vector for decarbonizing the current energy system, appearing in numerous studies where ultra-pure hydrogen can be reached thanks to highly selective membranes [9]. In this context, membrane technology is widely proposed to separate high-purity hydrogen and be directly used in internal combustion engines, turbines, or fuel cells [10,11], recover residual hydrogen from exhaust gases in the metallurgical industry [12], use the current natural gas infrastructure to storage and transport hydrogen [13,14], and intensify current production processes by the combination of chemical reaction and separation in a unique step thanks to membrane reactors [15,16], among other possibilities.

A wide variety of materials have been proposed for membrane fabrication, including both polymers and inorganic compounds. Polymers represent the cheapest option, sufficiently good processability, reproducibility, and versatility to be fabricated in different geometries. However, their thermal resistance and durability under certain complex gas mixtures containing certain impurities, and relatively low H₂-selectivity limit their practical applications [17,18]. These limitations can be almost completely overcome by using inorganic membranes with both porous and dense structures that provide good performances in terms of permeate flux and H₂-selectivity for wider intervals of operating conditions at the expense of their higher cost [19].

Even though porous inorganic materials such as zeolites [20,21] or carbon structures [22,23] have provided promising results for such applications, dense structures made of perovskites [24,25] or certain metals like palladium or its alloys [26,27] still prevail in the literature. Particularly, the complete theoretical H₂-selectivity and versatility of Pd-based membranes against most conventional operating conditions have

extended their use during the last decade [28,29]. The high cost of the palladium and inversely proportional dependence of permeate flux with thickness have promoted the preparation of composite membranes in which a fully dense but very thin Pd-film is deposited onto the surface of porous substrates that provide the required mechanical integrity [30,31]. Both porous ceramic and metallic supports are typically used for this purpose, although a definitive solution has not been adopted. On the one hand, the ceramic supports offer excellent surface properties in terms of high porosity, low average pore size, narrow pore size distribution and smooth surface. On the other hand, the metallic supports ensure better assembly into conventional industrial devices (usually made of stainless steel), reduction of possible intermetallic diffusion at high temperatures and expect longer-time operation against thermal cycles due to their closer thermal expansion coefficients [32,33]. For this reason, both alternatives can be combined by modifying by incorporating diverse materials onto porous metallic supports with aim to improve their surface quality. The idea is to set it as much closer as possible to the reached with the ceramic supports but maintaining the main benefits of using a metal core. In this context, the incorporation of many different ceramic particles between porous metal supports and Pd-films has demonstrated the possibility of reaching relatively low Pd-thickness below 15 μm, good membrane performance and resistance in independent purification or membrane reactor applications [34,35]. In all these cases, palladium deposition is frequently carried out by Electroless Plating or related variants due to its simplicity, low energy requirements and the possibility to cover homogeneously complex conducting and non-conducting geometries [30]. In particular, the alternative denoted as Electroless Pore-Plating (ELP-PP) provides excellent performance in terms of mechanical resistance of the sandwich-type composite structure even in case of working under tensile stress while minimizing the number of rejected membranes during their fabrication [36].

Due to the multiple available strategies for the fabrication of Pd-based composite membranes and good preliminary performance for most of them, the evaluation of other complementary criteria is of key importance, supporting their definitive penetration in the industry. Among them, both economy and environmental impacts can be highlighted as powerful tools helping to decide the best fabrication strategy. Much of the research published in specialized literature does not consider any economic aspect so, despite their technical achievements, the transferring to the industrial sector can become a tortuous path. Something similar occurs in terms of environmental sustainability, despite the increasing concerns in this matter. In this context, Life Cycle Assessments (LCA) can be applied as a rigorous method to determine and quantify the major environmental impacts generated during the fabrication of membranes [37]. This methodology analyzes all processes involved in the fabrication of membranes, quantifying the entire set of material and energy inputs/outputs to determine their effects on both environment and human health under standardized procedures ISO-14040 and ISO-14044 [38]. Di Marcobernardino et al. [39] applied these tools

to analyze the potential economic and environmental benefits reached while replacing a traditional process scheme by using of a membrane reactor to produce pure hydrogen from biogas and bioethanol. However, to the best of our knowledge, precise information about the environmental impacts directly coming from the fabrication of H₂-selective membranes, especially Pd-based supported membranes, is very scarce in the literature. In fact, only a preliminary LCA focused on ELP-PP Pd-membranes has been recently published to demonstrate the benefits of incorporating a ceramic intermediate layer between the PSS support and the H₂-selective Pd-film [40]. In the study, precise experimental data about the fabrication process were used to account for both materials and energy requirements, appearing the palladium deposition as the most contaminant manufacturing step due to both required metal and high-energy consumptions. Therefore, the use of any PSS support modification, i.e., the incorporation of an intermediate layer formed by CeO₂ particles, could help to reduce the final Pd-thickness and, hence, the associated environmental impacts. Based on these preliminary results, the current study goes into depth about this relevant insight by including cost analysis and influence of scaling-up the total membrane length in case of fabricating composite membranes with CeO₂-based intermediate layers. In this context, two novel fabrication alternatives with diverse types of ceramic particles as intermediate layer have been compared with the most promising one selected in our previous study, based on the incorporation of an intermediate layer made of raw dense CeO₂ particles. In this occasion, the original ceramic is replaced by porous CeO₂ or dense particles but doped with finely and well-distributed Pd-nuclei before their incorporation as intermediate layer. In all the cases, the effects on Pd-thickness and H₂-permeance are correlated with all associated environmental and economic issues. In addition, the study has been extended for the first time to the preparation of membranes with increasing lengths up to typical standard industrial sizes with the aim to select the most adequate dimension to minimize the environmental impacts during their fabrication. This new study provides a rigorous multi-factor criteria to select the most attractive strategy for fabricating composite Pd-membranes, particularly those prepared by ELP-PP, although these steps can be also applied to many other types of Pd-dense membranes or even different membrane types with some minor adaptations.

Experimental section

Membrane fabrication process

In this work, different tubular composite-membranes were fabricated onto AISI 316L porous stainless steel (PSS) supports from Mott Metallurgical corp. (Farmington, USA). These tubes present a symmetric structure with 0.1 μm porous media grade, an external diameter of 1.27 mm, and 0.20 mm wall thickness. A series of oxides and ceramic particles were incorporated onto the commercial supports as intermediate layer after an initial cleaning to reduce the original roughness and average pore size. In this context, the use raw dense CeO₂ particles as intermediate layer, selected in our previous study as better alternative than incorporating the palladium directly on the calcined supports [40] (here denoted as MB#01), is now compared with the use of two different CeO₂-based materials: porous CeO₂ (MB#02) and dense Pd-doped particles (MB#03), both maintaining analogous particle sizes of around 100 μm (Fig. 1).

Fig. 2 collects the general fabrication steps carried out for the preparation of all above-mentioned Pd-membranes. Independently of the selected fabrication strategy, certain steps are common for all the membranes. First, all raw PSS supports should be pre-treated (PT) by surface cleaning and calcination in the air at high temperatures [31,41]. The cleaning step is carried out by successive immersions in solutions of sodium hydroxide 0.1 M (PT-1.1), hydrochloric acid 0.1 M (PT-1.2), and ethanol 96 vol% (PT-1.3) under ultrasonic stirring at 60 °C (ultrasonic bath Selecta 6000138, 600 W), then being dried overnight at 110 °C (oven AX-30, 1000 W). After that, the clean supports were calcined in air at 600 °C (furnace CARBOLITE-MTF 12/25/250, 700 W) for 12 h with heating and cooling ramps of 1.8 °C min⁻¹ (PT-2). The last step, in which a fully dense palladium film is incorporated by Electroless Pore-Plating (ELP-PP) to purify gas streams containing hydrogen [41,42] with high selectivity, is also common for all the membranes. Basically, the plating process consists of feeding an ammoniacal solution containing the metal source and diluted hydrazine as reducing agent from opposite sides of the porous substrate, thus forcing the chemical reaction between them to take place just inside the pores or in their neighborhood (PD-1). This process is carried out at 60 °C (hotplate Selecta 7001512, 550 W) and repeated for several recurrences till all the pores become entirely closed and the

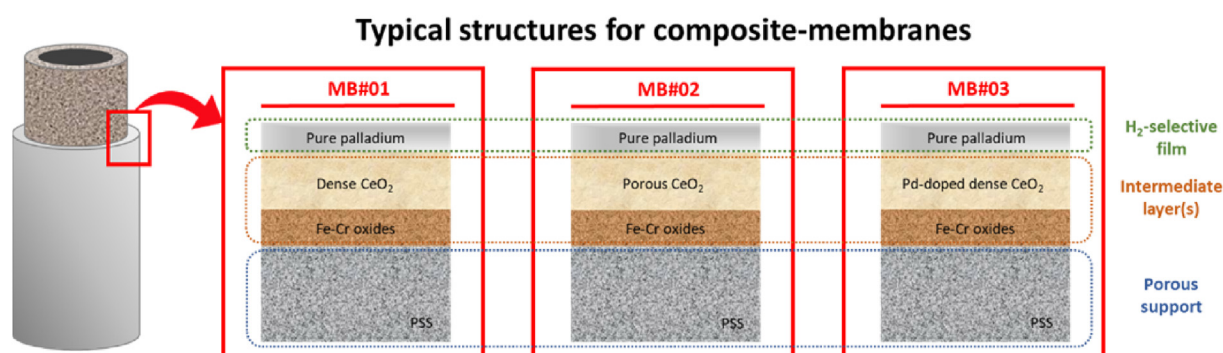


Fig. 1 – Cross-sectional scheme for each Pd-membrane considered in the present study.

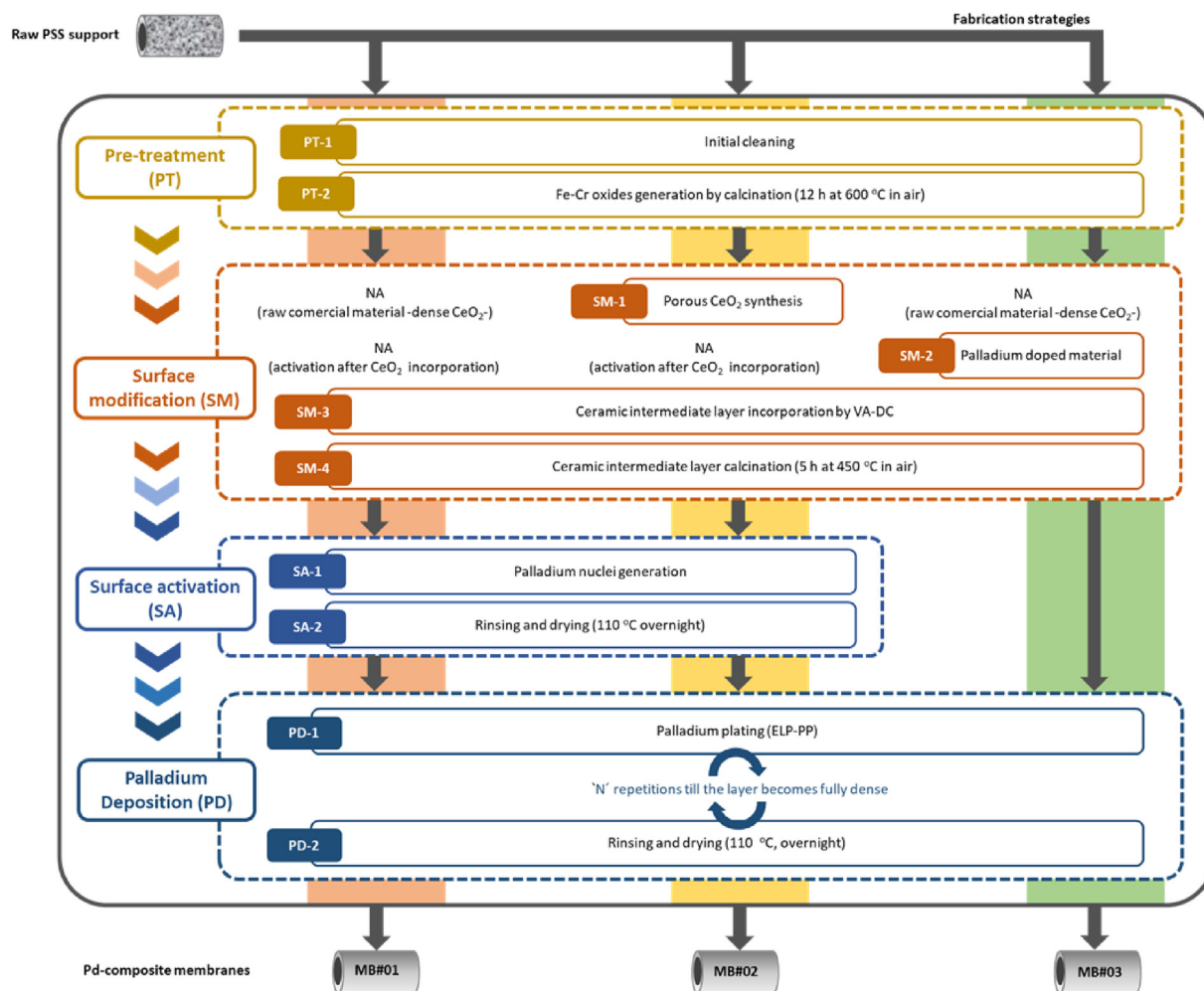


Fig. 2 – General fabrication steps performed for different Pd-membranes with CeO₂-based intermediate layers.

membrane turns non-permeable to any different gas to hydrogen, typically nitrogen or helium. Between each plating cycle, the membrane is rinsed with deionized water and dried overnight at 110 °C to ensure the penetration of the solutions into the remaining partially open pores during successive cycles (PD-2). In this context, it should be noted that the duration of the plating cycles usually increases from 2 to 7 h at the last stages to facilitate the contact between the solutions mentioned when the pores are nearly completely closed. After these common steps, the main fabrication differences between the membranes analyzed in the present study are related to the incorporation of the ceramic intermediate layer (SM) and the surface activation (SA) necessary before depositing the top Pd-film by ELP-PP to ensure adequate adherence and homogeneity.

The first membrane type, MB#01, already published in our previous work [40] and included here as a reference for easier comparison with the new ones, contains raw commercial and dense CeO₂ particles of around 100 μm as a ceramic intermediate layer. These particles are directly incorporated onto the external surface of pre-treated PSS supports by vacuum-assisted dip-coating (VA-DC) with help of a vacuum pump (ABM 4EKF63CX-4, 180 W) from a suspension containing 10 vol % of ceramic particles and 2 vol% PVA (SM-3). Next, the modified support calcined to remove the organic linker (SM-4)

before incorporating the palladium accordingly to the detailed process described elsewhere [42]. The synthesis and conformation of these CeO₂ particles are not considered for this particular membrane fabrication strategy due to its commercial availability at a reasonably low cost. In addition, the required surface activation (SA) with well-distributed fine palladium nuclei before the palladium deposition is carried out by two consecutive steps: i) contact of an acidic diluted solution of palladium chloride and a mixture of hydrazine 0.2 M with ammonia 2.0 M through the pores of modified supports for 2 h at room temperature (SA-1), and ii) rinsing with deionized water and drying overnight at 110 °C to ensure the complete removal of humidity from the pores (SA-2).

The second fabrication alternative, denoting the reached membrane as MB#02, maintains all the steps mentioned above but it incorporates a first additional one related to the synthesis of the ceramic intermediate layer material since it is certainly difficult to purchase this advanced porous material at a reasonable cost. Particularly, it is based on porous CeO₂ particles fabricated by nano-casting from a typical SBA-15 structure, as detailed elsewhere [36]. This synthesis procedure can be briefly described as the impregnation of typical SBA-15 with a suspension of cerium nitrate in ethanol till the entire pores of the material become filled by the precursor. Then, the solvent is

Table 1 – Concentration of chemicals used during the preparation of ELP-PP composite Pd-membranes (independently of the particular fabrication route).

PT Pretreatment	PT-1 Initial cleaning	PT-1.1		PT-1.2		PT-1.3	
		NaOH (g/L)	2.0	HCl 35% (mL/L)	2.0	C ₂ H ₅ OH 96% (mL/L)	1000
	PT-2 Oxides generation	n/a					
SM Surface modification	SM-1 CeO ₂ synthesis	SM-1.1		SM-1.2		SM-1.3	
		SBA-15 (g/L)	120	NaOH (g/L)	2	C ₂ H ₅ OH (mL/L)	1000
		Ce(NO ₃) ₃ (g/L)	97				
		C ₂ H ₅ OH (mL/L)	1000				
	SM-2 CeO ₂ doping	SM-2.1		SM-2.2			
		PdCl ₂ (g/L)	0.1	NH ₄ OH 32% (mL/L)	120		
		HCl 35% (mL/L)	1.0	N ₂ H ₄ (mL/L)	10		
	SM-3 CeO ₂ incorporation	SM-3.1					
		CeO ₂ (g/L)	100				
		PVA (g/L)	20				
SM-4 Calcination/PVA removal	n/a						
SA Surface activation	SA-1 Pd nuclei generation	SA-1.1		SA-1.2			
		PdCl ₂ (g/L)	0.1	NH ₄ OH 32% (mL/L)	120		
		HCl 35% (mL/L)	1.0	N ₂ H ₄ (mL/L)	10		
	SA-2 Rinsing and drying	n/a					
PD Palladium deposition	PD-1 Pd plating (ELP-PP)	PD-1.1		PD-1.2			
		PdCl ₂ (g/L)	5.4	N ₂ H ₄ (mL/L)	10		
		NH ₄ OH 32% (mL/L)	390				
		Na ₂ EDTA (g/L)	70				
	PD-2 Rinsing and drying	n/a					

evaporated, and subsequent transformed the cerium nitrate into CeO₂ by calcination in air at high temperature. The procedure is typically repeated at least 3 times to ensure a complete impregnation of all the pores of SBA-15 powders and reach a high-quality nano-casted material. The complete removal of the hard temporary silica-based template is carried out by two consecutive washing steps in aqueous NaOH solutions (2.0 M) under stirring at 300 rpm and 60 °C for 4 h, sedimentation overnight at static conditions at room temperature, and vacuum filtration to recover the solid material. Finally, the new porous CeO₂ particles are rinsed with deionized water, ethanol, and acetone several times and dried overnight at 120 °C.

The last fabrication strategy is based on modifying CeO₂ particles used as an intermediate layer before their incorporation onto the porous support by VA-DC, denoting the resulting membrane as MB#03. Particularly, commercial dense ceramic particles are considered, so their synthesis and conformation do not apply in this case. However, in contrast to the general procedure previously described for the fabrication of MB#01, these particles are doped with fine and well-distributed Pd nuclei before their coating onto the substrate (SM-2), thus avoiding the necessity of performing an additional surface activation just before the palladium deposition by ELP-PP. Further experimental details about this fabrication strategy can be found in our previous work [43].

In all these cases, each step requires the use of different chemicals, materials, water, and electricity that entail a

certain environmental footprint. To be precisely determined in the dedicated section of this study (section Materials inventory for membranes preparation), Table 1 collects here all precise concentrations of each required chemical used during the membrane fabrication, independently to the particular route followed during its preparation. All different solutions and suspensions are always balanced in water, thus not including with detail in the table the water content. Moreover, it should be noted that certain steps do not consume any chemical due to their nature, mainly based on cleaning or thermal processes at moderate or high temperatures. This fact occurs for the generation of a first intermediate layer based on Fe–Cr oxides (PT-2), the PVA removal after incorporation of the ceramic intermediate layer (SM-4) and rinsing/drying steps performed after the activation with Pd nuclei (SA-2) or the palladium incorporation by ELP-PP (PD-2).

Fundamental membrane characterization

The fundamental characterization of any Pd-based membrane always includes morphological analyses to evaluate the homogeneity of all stacked layers and the final Pd-thickness, which typically defines its permeation capacity and cost. In this study, a Kern electronic balance type ABS 220–4 (accuracy of ±0.001 g) and a scanning electron microscope Hitachi S–2100 N equipped with an X-ray diffraction system are used for these purposes. Moreover, the particular performance of the

membranes needs also to be determined through permeation measurements under diverse operating conditions. Thus, typical parameters such as permeate flux, H₂-permeance, selectivity to hydrogen, or activation energy, among others, can be determined to select the most suitable application for each membrane and design the appropriate modules. These tests are performed in a specifically designed device in which the tubular membrane is placed between two graphite O-rings to ensure proper sealing between both the retentate and the permeate sides [36,44]. At the same time, the desired temperature for experiments is reached by an electric furnace around the permeation cell. The permeate side is always maintained at atmospheric pressure, setting a specific pressure difference across the membrane thanks to a Bronkhorst EL-PRESS back-pressure regulator in the retentate side with a capacity ranging from 0.1 to 10 bar. Feed streams are regulated by individual Bronkhorst EL-FLOW mass flow controllers with a maximum capacity of 400 NmL min⁻¹, while permeate and retentate streams are analyzed with a high-precision Horiba film flowmeter with a minimum detection limit of 0.2 mL min⁻¹.

Life cycle assessment (LCA) methodology

LCA methodology aims to quantify the environmental impacts of a product or service over its entire life cycle [45,46]. The LCA analysis presented in this study was conducted under ISO-14040 [47] and ISO-14044 [48] standards, which describe the general methodological principles and framework to perform the analysis, in addition to some useful guidelines and good practices. In this manner, the LCA analysis presented in the current study is used to determine unequivocally the effects of each material and energy input/output required or produced, respectively, during the manufacturing of composite ELP-PP membranes on both environment and human health.

LCA goal and scope

The main goal of the current LCA, carried out on diverse strategies for the fabrication of composite ELP-PP Pd-membranes, is multi-fold, addressing the following issues.

1. Identification of critical synthesis stages with the highest environmental impacts for each analyzed membrane fabrication route, thus compromising the long-term feasibility of the process.
2. Comparison of reached results for each alternative at a lab-scale to use the proposed methodology as an additional tool to select the most suitable strategy together with the membrane performance. The functional unit selected for the study is a concrete membrane permeation area of 100 cm² considering different fabrication batches for obtaining a total area of around 400 cm², equivalent to 33 membranes of 3 cm in length.
3. Finally, the most promising alternative determined in the previous analysis will be scaled-up for longer membrane lengths up to 100 cm to analyze the eventual environmental implications of fabricating membranes on a real industrial scale, thus predicting a more realistic scenario. For this purpose, the selected functional unit will be maintained as 100 cm² of membrane permeation area,

considering different fabrication batches for obtaining a total area of around 400 cm², independently of the addressed membrane length. At this point, it should be mentioned that the study is based on actual experimental data at a lab-scale for diverse membrane dimensions up to 25 cm in length, estimating the required supplies for longer sizes due to certain limitations in the available facilities.

For all different fabrication strategies addressed in the current study, the cradle-to-gate LCA scope starts with the provisioning of required raw materials for each step, from the PSS support pre-treatment to the Pd-deposition by ELP-PP. Therefore, all inputs and outputs required for the Pd membranes manufacture, including both materials and energy, were considered within the system boundaries. In all LCA scenarios, the use and end-of-life phase of the membranes are not considered since both issues are independent of the fabrication route. In addition, end-of-life treatment of membranes or other waste disposals generated during the fabrication process have not been included in the present study due to the absence of available and reliable data on both behavior and post-mortem treatment of the membranes or waste solutions after disposal. Moreover, it should be considered that solution not completely spent can be used for the preparation of diverse membranes (not necessarily in the same concrete step).

Life cycle impact assessment (LCIA)

SimaPro v8.1 has been considered to model the LCA by using complete inventory data for each case addressed in the study, which has been further provided as supplementary material. The environmental performance assessment of the proposed manufacturing strategies and scale-up has been carried out through the ReCiPe mid-point methodology in the hierarchical perspective [49]. This methodology provides direct insight into the cause-effect chain of an impact category [49,50], while it seems to be suitable for LCA analyses on composite Pd-based membranes for different purposes [51,52]. Finally, it should be noted that the complete list of analyzed impact categories is also collected as supporting information for possible revision, including the manuscript core only the most relevant impacts: climate change (CC), human toxicity (HT), acidification (AC), freshwater ecotoxicity (FWE), metal depletion (MD) and fossil fuel resources depletion (FD).

Cost analysis

Additionally, a cost analysis for each fabrication route has been also included in the current study as relevant criteria to support the selection of the most promising alternative. As main operating expenses for each case, the cost of porous supports (PSS), chemical reactants (palladium source and other chemicals) and electricity have been considered in the basis of budgets within the period 2020–2021, in which all the membranes were prepared. In this context, as example, an average annual cost in Spain of around 0.14 €/kWh has been considered for electricity [53]. The current inflationary trend for prices caused by geopolitical instability between Russia and Ukraine has not been considered due to its expected relatively transient nature. Moreover, the associated capital expenses, amortization of required devices and labor costs are

neither included in this study, considering the necessity of a similar budget for these concepts, independently of the selected fabrication strategy.

Results and discussion

Fundamental membrane characterization

Morphological characterization and permeation behavior of composite membranes is typically analyzed to understand the progressive membrane formation during the fabrication process. Among all of them, the final analyses define the membrane performance, and they are taken as a reference to compare various membranes. The three ELP-PP membranes included in the present work were fabricated following a similar strategy, as previously addressed, with the unique

variation of incorporating three different CeO_2 -based intermediate layers. These barriers are formed by raw dense (MB#01), porous (MB#02), or Pd-doped dense (MB#03) CeO_2 particles, being described in detail in our previous works [36,42,43]. To summarize all their main characteristics together and facilitate the subsequent discussion in terms of environmental and cost impacts, Fig. 3 collects some relevant micrographs of both the final surface and cross-section reached after the incorporation of palladium for each case. In general, a very similar external surface is achieved after the palladium incorporation onto each modified porous support by ELP-PP, independently of the characteristics of the CeO_2 particles. Thus, an almost continuous Pd-film is always generated, covering the entire external surface of the supports (Fig. 3a, c and d). This morphology is typical of other ELP-PP membranes due to the pass of hydrazine through the biggest pores of the supports despite the chemical reaction preferentially starts

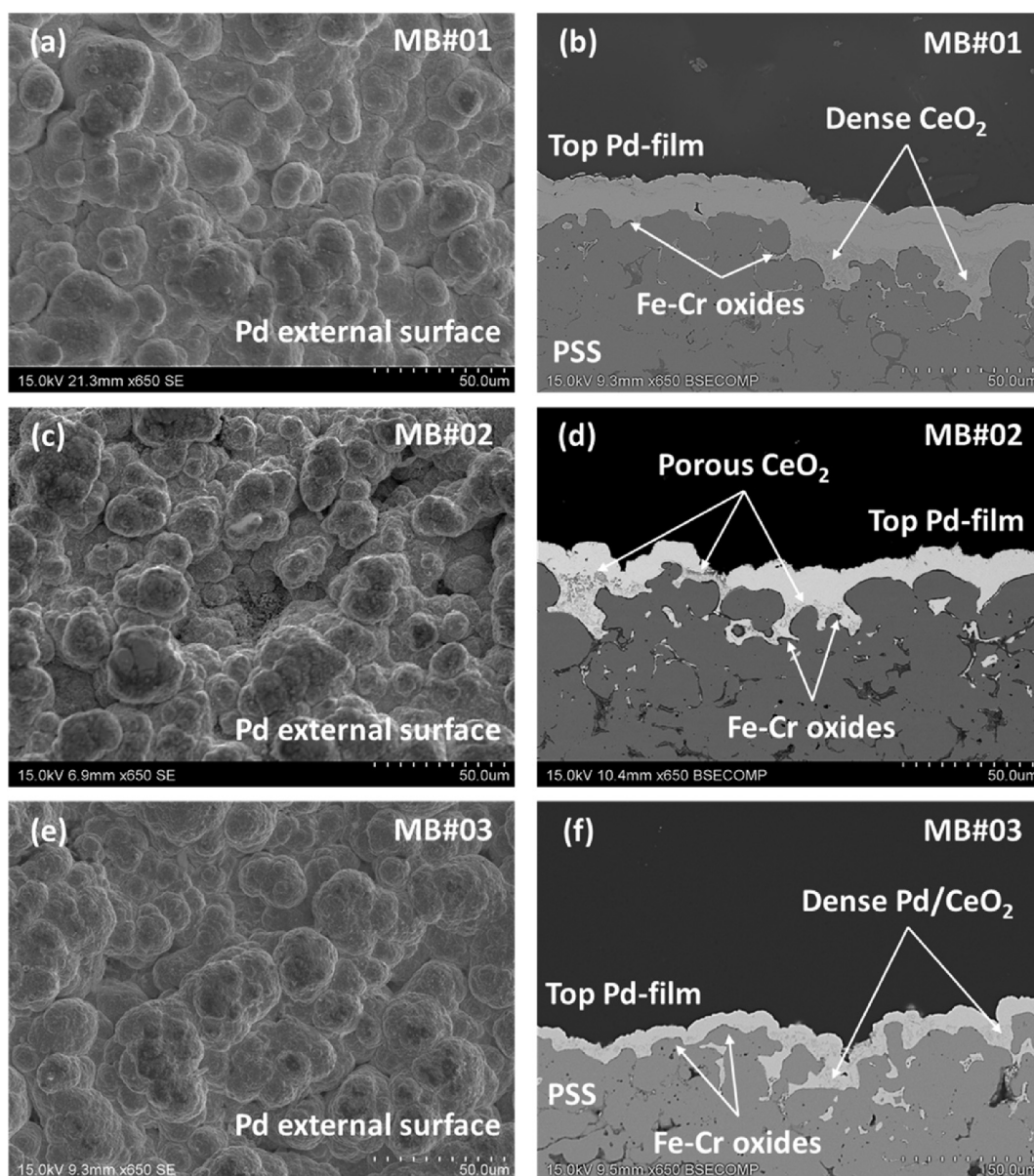


Fig. 3 – SEM images of the external surface (left column) and cross-sectional (right column) for Pd-membranes prepared with different CeO_2 -based intermediate layers: raw dense (a,b), porous (c,d), and Pd-doped dense (e,f) particles.

just around the smaller pores [44]. However, a completely continuous external film is not required to obtain high H₂-selectivity due to the nature of the ELP-PP deposition process, being enough the complete blockage of all the substrate pores by palladium. In fact, some residual external pores or cavities can be also distinguished in these membranes, although the absence of bubbles has demonstrated their complete tightness in helium up to 3 bar during leak tests with ethanol at room temperature. This fact indicates that these remaining external pores are not interconnected, and the membrane fabrication can be considered complete.

More significant differences between the samples appear when analyzing the cross-sectional views (Fig. 3b, d and f), in which the final thickness of the external Pd-film clearly depends on the material used as the intermediate layer. Thus, the thicker external layer is generated after incorporating commercial raw and dense CeO₂ particles as intermediate barrier (MB#01), being necessary around 15 μm of palladium to obtain a fully dense membrane (Fig. 3b). The incorporation of the ceramic intermediate layer on the deepest and largest pores and the relatively thick Pd-film moderate the original surface roughness of the PSS support, as widely discussed in our previous work [42]. Moreover, a certain infiltration of palladium inside the closest pores to the external surface can also be appreciated as it typically occurs in other membranes fabricated by ELP-PP. However, using porous ceramic particles as an intermediate layer to reduce the thickness of the top Pd-film in the range 7–12 μm and reach a fully dense membrane (MB#02, Fig. 3d). In this case, the ceramic particles partially block the largest pores of the PSS support, reducing both original porosity and roughness in a similar manner that occurs when applying raw dense particles. Nevertheless, the further internal porosity of ceramic particles facilitates the contact between the hydrazine and the palladium source inside the support pores, making it possible to reach their complete blockage with a minor amount of the noble metal. Because of the lower palladium thickness, the final top Pd-film replicates in better manner the surface of the modified support [36]. A similar effect was achieved by doping the dense CeO₂ particles with Pd-nuclei before their incorporation on the PSS support as intermediate layer (MB#03, Fig. 3f), thus replacing the conventional activation step that was always required before the electroless plating. As can be seen on the cross-sectional image, a very homogeneous top Pd coating with a thickness of around 9 μm is obtained by following this synthesis strategy, also detecting a certain amount of infiltrated palladium inside the pores near the external surface of PSS tubes [43]. In this context, it is also important to highlight that diverse fabrication batches were completed for each membrane type, maintaining very similar morphological properties in more than 20 different samples. This fact ensures good reproducibility of the membrane fabrication process, even after progressively increasing the total membrane length up to 25 cm. Pd-thicknesses within the ranges mentioned above were also obtained for these longer membranes, not detecting differences of the top Pd-film and metal infiltration inside the pores along the axial direction in a noticeable manner.

Once a general overview of the morphological properties of studied membranes is presented, it is also useful to summarize their main permeation properties in terms of permeate fluxes,

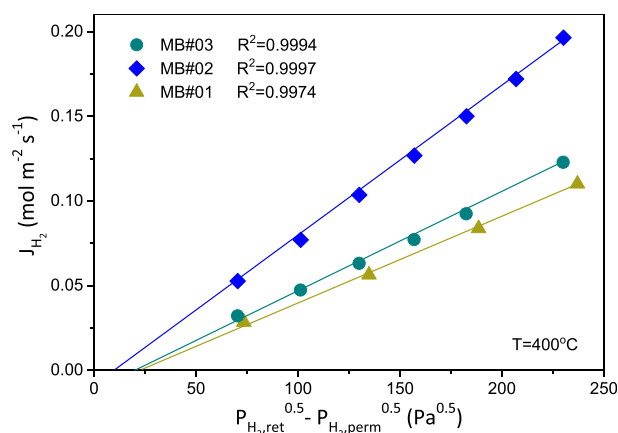


Fig. 4 – Permeation behavior of ELP-PP membranes containing diverse CeO₂-based intermediate layers (T = 400 °C).

permeance, and H₂-selectivity. First, it should be noted that no nitrogen was observed in the permeate side for the entire set of permeation experiments carried out at high temperatures (minimum detection limit of 1.67·10⁻² mL min⁻¹), thus ensuring a complete gas tightness to other species different to hydrogen and an ideal H₂/N₂ separation factor (α_{H_2/N_2}) greater than 10,000. In these conditions, Fig. 4 collects the H₂ fluxes obtained in the permeation experiments carried out at 400 °C for pressure driving forces in the 0.25–2.50 bar range. A direct relationship between Pd-thickness and permeation can be deduced from these results, obtaining a lower permeation as the Pd-thickness increase, as predicted by the Sieverts' law. Thus, the membrane MB#01 with around 15 μm thick top Pd-film and including an intermediate layer formed by commercial raw and dense CeO₂ particles exhibits the lowest permeation capacity, with a H₂-permeance of 5.37·10⁻⁴ mol m⁻² s⁻¹ Pa^{-0.5}. This value increases in case of replacing the intermediate layer by porous CeO₂ (MB#02) or Pd-doped dense CeO₂ particles (MB#03) up to 1.03·10⁻³ and 6.26·10⁻⁴ mol m⁻² s⁻¹ Pa^{-0.5}, respectively. At the same time, the average Pd-thickness is reduced to around 10 μm, as previously discussed. Here, it should be noted that higher permeation fluxes are reached in case of considering the use of porous ceramic particles as intermediate layer despite their slightly higher average Pd-thickness in comparison to the obtained one while using Pd-doped dense particles. This fact can be justified by the presence of internal pores in the ceramic particles that reduce other mass transfer resistances, thus facilitating the hydrogen permeation through the composite membrane.

Analyzing in detail the experimental data obtained from these experiments, the linear relationship between H₂ permeation fluxes and pressure driving forces for the process is straightforward, thus suggesting that H₂-diffusion through the Pd-film is the rate-determining step, as expected for most Pd-composite membranes [54,55]. However, none of these experimental data fitting intercepts in (0,0), as suggested by the traditional Sieverts' law. This peculiarity has been previously reported in many other Pd-based membranes fabricated by ELP-PP, justified by the palladium infiltration inside certain pores near the external surface of the support where the Pd-film is generated during the plating process [30,44,56].

Table 2 – Pd-thickness and H₂-permeance reached in ELP-PP membranes containing diverse CeO₂-based intermediate layers.

Sample	Membrane morphology			Permeation behavior	
	Ceramic Intermediate layer	Pd-thickness (μm)	Variation (%)	k _{H2} (mol m ⁻² s ⁻¹ Pa ^{-0.5})	Variation (%)
MB#01	Raw dense CeO ₂	15	–	5.37 · 10 ⁻⁴	–
MB#02	Porous CeO ₂	10	- 33	1.03 · 10 ⁻³	+91
MB#03	Pd-doped dense CeO ₂	9	- 40	6.26 · 10 ⁻⁴	+17

Although this partial infiltration improves the adherence of the Pd-film and, hence, the mechanical resistance of the membrane, also turns the calculation of real pressure driving forces difficult just onto the contrary surfaces of the palladium layer, as it should be considered to make use of the Sieverts' law [44]. In this manner, the partial deposition of palladium inside the pores of the support generates a tortuous surface of the Pd film just in contact with the support and partial hydrogen pressure on this side differs from the measured value in the bulk gas phase, thus introducing a certain uncertainty on the expression given by Sieverts' law [36].

To provide a general overview of the main properties obtained for the different membranes considered for the current study and facilitate their comparison, Table 2 details both Pd-thickness and H₂-permeance for each case, also including the variation of these parameters when porous or Pd-doped particles replace raw commercial and dense CeO₂ in the considered intermediate layers.

Materials inventory for membranes preparation

This section collects the complete inventory for materials and energy required for each fabrication step, later considered to perform the environmental impacts assessment and economic analysis. This information is presented in four different groups corresponding to the following fabrication steps: pre-

treatment (PT), surface modification (SM), surface activation (SA) and palladium deposition (PD). Table 1, previously discussed, contains the precise details about all chemical reactants and particular composition for each solution, as required to prepare the addressed composite membranes in the study (see detailed procedures in previous experimental section). Table 3 here included complements the previous given information about materials with the total number of cycles finally required for each fabrication step and the spent volume of each solution per cycle, thus being possible to determine the total amount of each material used during the membranes' fabrication. Here, it should be noted that the selected nomenclature distinguishes between the unnecessary concrete steps for a certain fabrication strategy (indicated as not applicable, n/a) and the cases in which the steps lack any material consumption (denoted with dash). In example, all the steps based on drying or calcinating samples (PT-2, SM-4) do not require any material, so they are omitted from the material inventory. The initial cleaning of the supports (PT-1) involves the use of three different solutions (PT-1.1, PT-1.2 and PT-1.3) and a certain amount of distilled water for intermediate rinsing of the samples, being necessary to complete only one cleaning sequence to remove all possible pollutants from the commercial supports. The surface modification (SM) includes three different steps consuming materials that differ for each membrane considered in this study.

Table 3 – Inventory for materials and energy required during the preparation of each different membrane type (referred to the functional unit).

Fabrication steps	Materials	Different membrane types (L = 30 mm)										
		MB#01			MB#02			MB#03				
		Cycles	V (mL)	Electricity (kWh)	Cycles	V (mL)	Electricity (kWh)	Cycles	V (mL)	Electricity (kWh)		
PT	PT-1	PT-1.1	1	50	0.034	1	50	0.034	1	50	0.034	
		PT-1.2	1	50		1	50		1	50		
		PT-1.3	1	50		1	50		1	50		
SM	PT-2	–	1	–	6.06	1	–	6.06	1	–	6.06	
		SM-1	SM-1.1	n/a	n/a	n/a	3	50	2.13	n/a	n/a	n/a
			SM-1.2				1	50				
SM-1.3					1	50						
SA	SM-2	SM-2.1	n/a	n/a	n/a	n/a	n/a	n/a	1	50	–	
		SM-2.2							1	3		
		SM-3	SM-3.1	1	12.5	–	1	12.5	–	1	12.5	–
SA	SM-4	–	1	–	3.29	1	–	3.29	1	–	3.29	
		SA-1	SA-1.1	1	50	–	1	50	–	n/a	n/a	n/a
			SA-1.2	1	50	–	1	50	–	n/a	n/a	n/a
PD	SA-2	–	1	50	0.88	1	50	0.78	–	–	n/a	
		PD-1	PD-1.1	12 ± 2	100 ± 40	1.16	8 ± 1	50 ± 20	0.85	7 ± 1	50 ± 20	0.68
			PD-1.2	12 ± 2	36 ± 6		8 ± 1	24 ± 3		7 ± 1	21 ± 3	
	PD-2	–	12 ± 2	600 ± 50	10.56	8 ± 1	400 ± 50	7.04	7 ± 1	350 ± 50	6.16	

Thus, the step SM-3 based on the incorporation of CeO₂ particles as an intermediate layer onto the calcined PSS supports is the only common one for all the evaluated alternatives. In contrast, the synthesis of CeO₂ particles (SM-1) or their doping with Pd-nuclei (SM-2) are only used in some cases (MB#02 and MB#03, respectively). Some of these steps must be repeated for several times, as detailed in the table. Something similar occurs for all the steps involved in the surface activation (SA), which only apply for membranes MB#01 and MB#02. It is important to highlight that all materials have been considered for the analysis of the environmental impacts, independently of being synthesized in lab or directly purchased. Thus, all environmental impacts related to the use of CeO₂ and SBA-15 have been taken into account in our study. This includes available values from ecoinvent database about the metal extraction from the pit, the formation of oxide compound, and the impact of transportation to destination, among others.

Finally, the palladium deposition process (PD) is common for all the analyzed membranes, only varying the total number of ELP-PP recurrences necessary to reach fully dense membranes for each case. This variation is mainly caused by different surface properties of the supports while incorporating various CeO₂-based intermediate layers. However, it should be mentioned that other external reasons could provoke an increase in the spent volume of each solution. Thus, reusing a unique solution for all ELP-PP cycles is not always possible due to its occasional degradation, generating a certain uncertainty in the indicated spent volume. It can be produced by many different and unexpected operating troubles like deviations in the control of temperature or direct contact between the solution and screws used for the membrane assembly in the deposition cell, typically covered by Teflon. These issues are only observed on rare occasions, so these deviations are not considered for further use of the material inventory. On the other hand, it should be

highlighted that the final properties of analogous membranes were almost constant in terms of Pd-thickness, with an average deviation below 10%, being possible to assume a good reproducibility of the analyzed fabrication processes and the validity of collected data.

On the other hand, the energy consumption for each step has been also included here as electricity by considering both device power and time of usage. In general, most of these energy requirements came from all the steps in which an increase on the temperature is demanded (i.e., drying and calcination steps, plating cycles, etc.), although other operations such as rotation or the use of a vacuum pump have been also taken into account.

Environmental performance: LCA results

The strategical analysis of alternatives included in this study for preparing pore-plated membranes methods containing various CeO₂ materials as intermediate layer should also be considered by attending their environmental impacts. In this manner, both membrane morphology and performance under operation need to be analyzed together with the overall fabrication process sustainability to select the most adequate strategy to prepare these membranes in an expected wide application at an industrial scale. For this reason, Fig. 5 collects the most relevant environmental impacts generated during the fabrication, at laboratory scale, of composite membranes containing porous (MB#02) or dense Pd-doped CeO₂ particles (MB#03) as an intermediate layer in comparison to use raw commercial and dense CeO₂ particles (MB#01). The last membrane has been selected as a reference due to its noticeable lower environmental impacts in comparison to avoid any ceramic intermediate layer, as published in our previous work [40]. Therefore, the relative variation of each main environmental impact after replacing the raw dense

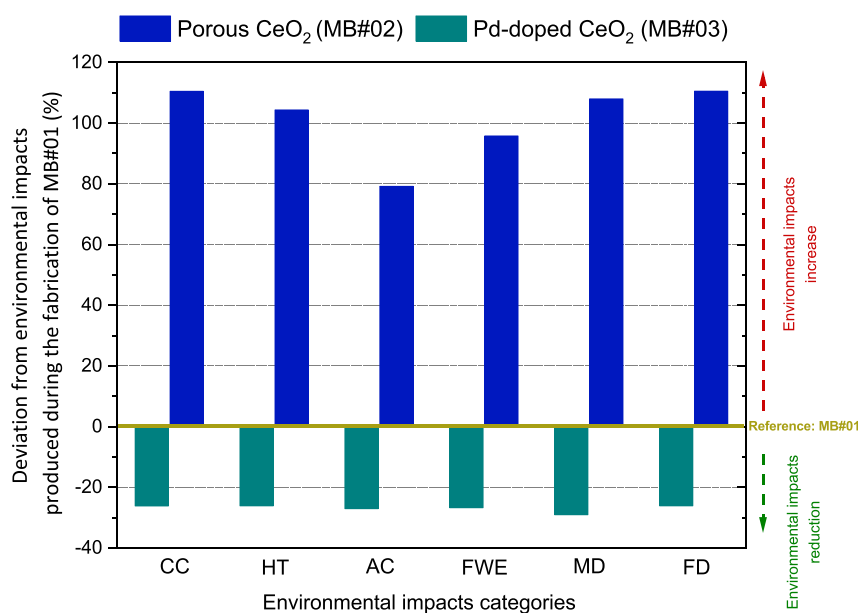


Fig. 5 – LCA results for laboratory scale preparation processes related to MB#02 and MB#03 membranes respect to the main environmental impacts generated in the preparation of MB#01: Climate Change (CC), Human Toxicity (HT), Acidification (AC), Freshwater Ecotoxicity (FWE), Metal Depletion (MD) and Fossil Fuel Depletion (FD).

CeO₂ particles of the intermediate layer by the alternatives mentioned above is represented in the figure. Detailed data for each environmental category has been generated after applying the ReCiPe mid-point methodology, collecting in detail all specific information about them (numerical and percentage form) in [Table S1](#) and [Figs. S1 of Supplementary Information–S2](#). Moreover, Monte-Carlo uncertainty analysis has been also included in this supplementary information to demonstrate the coherence of the values collected from the LCA analysis ([Figs. S3–S5](#)).

As can be seen, the fabrication of the membrane denoted as MB#02 and containing porous CeO₂ particles as intermediate layer generates a noticeable increase for all main environmental impacts categories in comparison to the reference membrane MB#01, in which raw commercial and dense CeO₂ particles were deposited as intermediate layer between the calcined PSS support and the H₂-selective Pd-film. On the contrary, the generation of an intermediate layer containing Pd-doped CeO₂ particles (MB#03) reduces the environmental damage generated during the fabrication process by an average of 27% in the selected impact categories. These results agree with the relative contribution of all steps required for the entire fabrication process when following each alternative. Detailed contribution of each synthesis step carried out to prepare MB#02 and MB#03 membranes are included as supplementary material for their eventual inspection ([Figs. S1 and S2](#), respectively), while those relative to the membrane taken as reference (MB#01) can be found in our previous publication [40]. The comparison of environmental impact uncertainty for these new membranes (MB#02 and MB#03) has also been added as supplementary information to reinforce the summary of results collected in [Fig. 5](#).

As previously addressed, the generation of an intermediate layer formed by porous CeO₂ particles (MB#02) clearly improves the permeance of the resultant composite membrane in comparison to the use of raw and dense particles. However, the high associated environmental costs could probably punish this synthesis strategy at an industrial scale. This environmental deterioration is mainly due to the fabrication step denoted as SM-1, which accounts around 60% of each selected impact (see [Fig. S1](#)). In this step, the surface modification of the PSS support is carried out to reduce original pore sizes and roughness. In this context, the generation of CeO₂ particles with an internal porosity is reached by nanocasting, which involves the use of commercial SBA-15 together with the cerium metal source and calcination at 600 °C to minimize the presence of defects in the new ceramic material that causes an increase in both materials and energy consumption. This fact avoids the great reduction of environmental impacts achieved after decreasing the required ELP-PP cycles from thirteen to eight into an overall improvement. On the contrary, the use of Pd-doped CeO₂ particles as an intermediate layer in MB#03 was globally reduced due to the greater importance of ELP-PP cycles reduction against the generation of Pd-nuclei around the ceramic particles before their incorporation onto the membrane (see details in [Fig. S2](#)). Remarkably, the total number of recurrences required to obtain complete gas tightness when incorporating Pd-doped CeO₂ particles decreased from thirteen to seven compared to the required number of ELP-PP cycles in the case of considering

raw CeO₂ particles as a ceramic barrier. As mentioned, these plating steps generate a relatively high environmental impact, mainly caused by the electrical consumption during drying steps between successive cycles. Therefore, reducing the total number of ELP-PP recurrences will provoke an associated time reduction during drying steps and, consequently, in the generated environmental impacts. Moreover, it should be considered that a lower number of ELP-PP recurrences also reduces the consumption of reagents, therefore contributing to a specific environmental improvement, although in a less significant way. In this case, the main step in which the surface of the support is modified (SM-2) does not involve any calcination. Thus, the environmental impact generated by this stage is almost negligible in comparison with the rest fabrication steps. At this point, it is necessary to point out the lab-scale of the membrane synthesis procedure considered for the present study until now. In this context, using more favorable production scales could reduce this contribution, replacing the electricity requirements of the electrical furnace with other alternatives well established in the industry (i.e., gas furnaces or solar energy).

In conclusion, all these experimental results demonstrate that the selected membrane fabrication strategy is crucial not only with the aim to improve the final membrane performance, mainly in terms of Pd-thickness and H₂-permeance, but also considering its sustainability and trying to minimize the associated environmental footprint. Both aspects can be misaligned, requiring adopting a compromise solution. Thus, using Pd-doped CeO₂ particles as an intermediate layer seems to provide certain benefits not only in the membrane performance but also in attending to environmental concerns.

Cost analysis

Together with the membrane performance and associated environmental impacts, the total cost for each fabrication route should also be relevant criteria to support the selection of the most promising alternative. However, this kind of analyses are very scarce in the available literature when comparing alternative fabrication strategies to reach supported membranes with limited Pd-thickness. Thus, [Fig. 6](#) represents the main operating expenses coming from using a porous support (PSS), different reactants (separating palladium from other chemicals) and electricity during the fabrication of diverse membrane types. These costs are referred to a single 3 cm in length membrane fabricated at laboratory scale, but assuming multiple batches to obtain a total permeation area of around 400 cm², as done for the environmental impacts.

All the considered values, detailed as supplementary information in [Table S2](#), come from accurate budgets managed during 2020–2021, in which all discussed membranes were prepared. An average annual cost for the electricity consumption of around 0.14 €/kWh has been considered taking into account that all the membranes were fabricated in Spain [53]. Here, the recent inflationary trend for prices caused by geopolitical instability between Russia and Ukraine has not been considered due to its expected transient nature. The consumption required for each of these items were collected in previous section Materials inventory for membranes

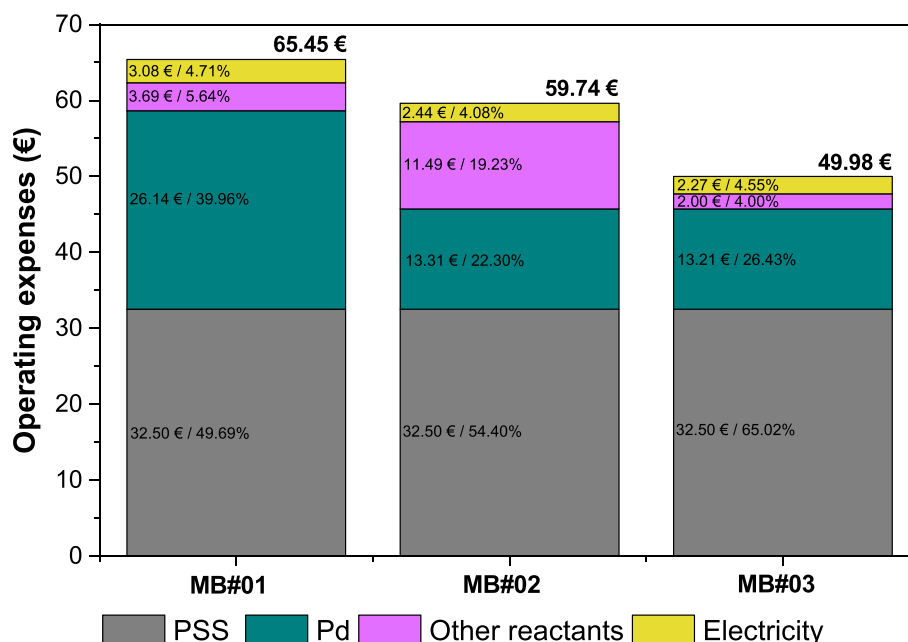


Fig. 6 – Cost distribution for main items required during the fabrication of ELP-PP membranes onto porous metallic supports (referred to a single membrane with 3 cm in length).

preparation dedicated to the material and energy inventories for the preparation of the membranes. On the other hand, the associated capital expenses, amortization of required devices and labor costs are neither included in this study, considering the necessity of a similar budget for these concepts, independently of the finally adopted fabrication strategy. Moreover, the lab scale considered for the analysis should always be in mind, assuming that certain savings could probably be produced while scaling up the fabrication technology. This particular effect will be later addressed in a specific section.

In this general context, some relevant insights can be extracted from the study. First, it should be noted that the PSS support cost is maintained constant for each membrane fabrication strategy because all of them are based in a common substrate with identical properties. In case of using dense or porous CeO₂ particles as intermediate layer without Pd-doping (MB#01 and MB#02, respectively), the support contribution to the overall cost of the membrane remains almost constant in the range 50–55%. In the first case, the other operating costs necessary to fabricate the membrane MB#01 are dominated by the required amount of palladium, with an average thickness of around 15 μm and contributing nearly 40% of considered operating expenses. Other materials, chemicals and electricity accumulate the remaining 10% to reach a total fabrication cost of 65.45 €. This cost contribution noticeably changes after replacing the raw dense CeO₂ by porous particles in MB#02. The associated cost to palladium is reduced in half due to the lower thickness required to obtain a fully dense film. However, the costs of other reactants and electricity drastically increase from around 10 to 23% due to the further fabrication steps required to synthesize the porous CeO₂ particles by nanocasting. Therefore, despite the noticeable reduction of the Pd-thickness reached in MB#02, the total cost of this membrane amounts to 59.74 €, only slightly reducing the reached one in case of considering raw dense

CeO₂ particles as an intermediate layer. On the contrary, the overall fabrication cost for the membrane MB#03, in which Pd-doped dense CeO₂ particles formed the intermediate layer, saves up to 24% of operating expenses to reach a final membrane cost of 49.98 €. In this case, the thickness reduction of the Pd-film from 15 to 9 μm due to the doping of dense CeO₂ particles used as an intermediate layer determines the savings due to the maintenance of similar cost derived from other items (PSS, electricity, and other reactants). Focusing on the distribution of new expenses, it should be highlighted that the porous substrate becomes the major contribution to the overall membrane cost (65%) and the palladium cost only represents around a quarter of the total amount. Therefore, greater efforts should be run to improve the original properties and associate costs of this type of porous metal substrates, which is very attractive to promote the penetration of these composite membranes in many industrial applications.

However, the membrane cost should be always considered together with the permeation capacity because higher permeation fluxes will require lower membrane area at analogous operating conditions. In this context, permeance of MB#02 is noticeably higher than MB#03, both improving the permeation capacity of MB#01 due to their lower Pd-thickness. However, MB#02 fabrication cost is only reduced below 10% while the associated environmental impacts almost double those generated for the referred material (MB#01). It can be justified, as previously mentioned, by the nanocasting steps carried out to generate the porous structure in the CeO₂ particles. On the contrary, MB#03 reduces both fabrication costs (in around 23%) and environmental impacts (in around 25%) while moderately increasing the H₂ permeance of the referred membrane. Thus, it is necessary to carefully analyze each particular case to find a compromise solution between the different alternatives. A new parameter is defined to correlate both permeance and fabrication cost as follows:

Table 4 – Materials inventory for the preparation of MB#03 with increasing tube lengths referred to the functional unit.

Step	Chemicals	Membrane length						
		30 mm ^a	50 mm ^a	70 mm ^a	110 mm ^a	250 mm ^a	500 mm ^b	1000 mm ^b
SM-1 (initial cleaning)	NaOH (g)	$2.50 \cdot 10^{-2}$	$2.50 \cdot 10^{-2}$	$2.50 \cdot 10^{-2}$	$3.30 \cdot 10^{-2}$	$5.00 \cdot 10^{-2}$	$1.00 \cdot 10^{-1}$	$2.00 \cdot 10^{-1}$
	HCl (g)	$2.98 \cdot 10^{-2}$	$2.98 \cdot 10^{-2}$	$2.98 \cdot 10^{-2}$	$3.97 \cdot 10^{-2}$	$5.90 \cdot 10^{-2}$	$1.19 \cdot 10^{-1}$	$2.38 \cdot 10^{-1}$
	EtOH (g)	9.86	9.86	9.86	13.15	19.72	39.45	78.90
	H ₂ O (g)	25.00	25.00	25.00	33.33	50.00	100.00	200.00
SM-3 (incorporation of CeO ₂)	CeO ₂ (g)	1.25	1.25	1.25	1.67	2.50	5.00	10.00
	PVA (g)	$2.50 \cdot 10^{-1}$	$2.50 \cdot 10^{-1}$	$2.50 \cdot 10^{-1}$	$3.33 \cdot 10^{-1}$	$5.00 \cdot 10^{-1}$	1.00	2.00
	H ₂ O (g)	12.50	12.50	12.50	16.67	25.00	50.00	100.00
PD-1 (activation with Pd nuclei)	PdCl ₂ (g)	$7.50 \cdot 10^{-4}$	$7.50 \cdot 10^{-4}$	$7.50 \cdot 10^{-4}$	$1.00 \cdot 10^{-3}$	$1.50 \cdot 10^{-3}$	$3.00 \cdot 10^{-3}$	$3.00 \cdot 10^{-3}$
	HCl (g)	$8.93 \cdot 10^{-3}$	$8.93 \cdot 10^{-3}$	$8.93 \cdot 10^{-3}$	$1.19 \cdot 10^{-2}$	$1.79 \cdot 10^{-2}$	$3.57 \cdot 10^{-2}$	$3.57 \cdot 10^{-2}$
	H ₂ O (g)	8.22	8.22	8.22	10.95	16.45	32.90	32.90
	NH ₄ OH (g)	$7.89 \cdot 10^{-2}$	$7.89 \cdot 10^{-2}$	$7.89 \cdot 10^{-2}$	$1.05 \cdot 10^{-1}$	$1.58 \cdot 10^{-1}$	$3.16 \cdot 10^{-1}$	$3.16 \cdot 10^{-1}$
PD-2 (Pd deposition by ELP-PP)	N ₂ H ₄ (g)	$7.50 \cdot 10^{-3}$	$7.50 \cdot 10^{-3}$	$7.50 \cdot 10^{-3}$	$1.00 \cdot 10^{-2}$	$1.50 \cdot 10^{-2}$	$3.00 \cdot 10^{-2}$	$3.00 \cdot 10^{-2}$
	PdCl ₂ (g)	$2.70 \cdot 10^{-1}$	$2.70 \cdot 10^{-1}$	$3.24 \cdot 10^{-1}$	$4.32 \cdot 10^{-1}$	$5.94 \cdot 10^{-1}$	1.24	2.43
	NH ₄ OH (g)	17.16	17.16	20.59	27.45	37.75	78.93	154.44
	Na ₂ EDTA (g)	3.50	3.50	4.20	5.60	7.70	16.10	31.50
	H ₂ O (g)	51.29	65.15	85.11	125.31	240.35	486.80	967.50
	N ₂ H ₄ (g)	$2.10 \cdot 10^{-1}$	$3.50 \cdot 10^{-1}$	$4.90 \cdot 10^{-1}$	$7.70 \cdot 10^{-1}$	1.75	3.50	7.00
PD-3 (cleaning and drying)	H ₂ O (g)	350.00	350.00	420.00	560.00	770.00	1610.00	3150.00

^a Laboratory values.

^b Estimated values.

$$M = \frac{\text{membrane cost}}{\text{permeance}} \left(\frac{\text{€}}{10^{-4} \text{mol m}^{-2} \text{s}^{-1} \text{Pa}^{0.5}} \right)$$

This parameter should be as low as possible, indicating the most favorable manner to reach a certain permeate flux. Excluding the cost of the support for this calculation (common for all the alternatives), parameter M decrease in half from the reference value $M = 6.14$ in MB#01 for the new proposed membranes. Particularly, M values of 2.64 and 2.74 are obtained for MB#02 and MB#03, respectively. As can be

appreciated, despite the marked difference in permeation capacity for both membranes, the relationship between cost and permeance is maintained almost constant. On the contrary, associated environmental impacts become noticeably higher in case of using porous ceria as intermediate layer for the membrane preparation. This fact suggests the use of Pd-doped and dense CeO₂ particles as intermediate layer instead of particles with complex porous structures to combine good membrane performance, low environmental impacts, and limited fabrication costs. For this reason, the

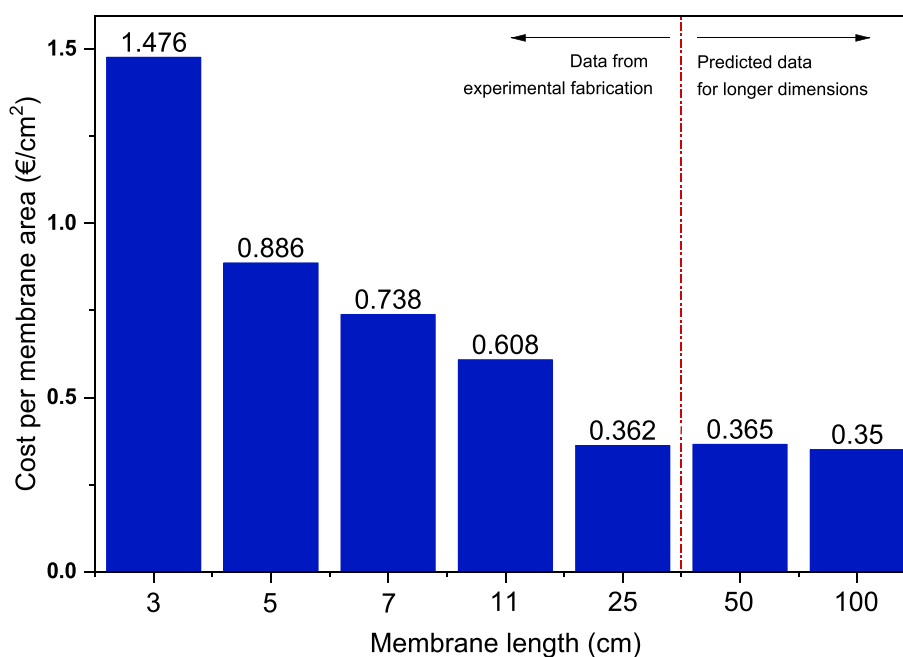


Fig. 7 – Variation of the membrane fabrication cost during scaling-up the membrane length.

membrane MB#03 has been selected to analyze in detail the effect of scaling-up its fabrication in next section.

Scaling-up the membrane fabrication

Once main concerns about membrane performance, environmental impacts and fabrication cost have been analyzed at laboratory scale, the effect of scaling-up their fabrication has

been also studied. As mentioned, it has been done in the case of using Pd-doped and dense CeO_2 particles as an intermediate layer before incorporating the top Pd-film onto PSS supports (MB#03). In this context, new analogous membranes but increasing their total length from 3 to 25 cm have been experimentally fabricated. First, it is necessary to point out that previously discussed membrane morphology in terms of homogeneity, roughness and average Pd-thickness is

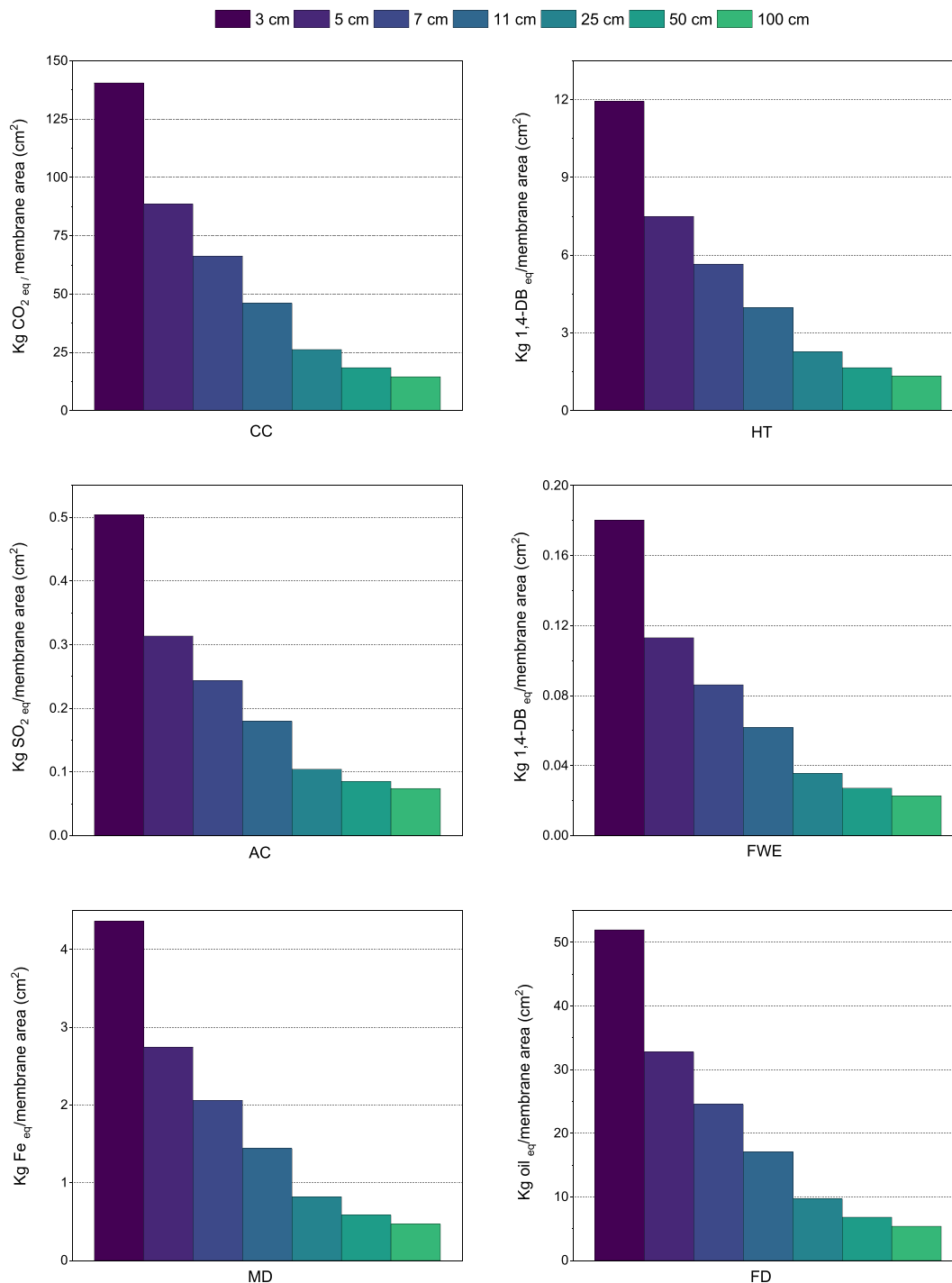


Fig. 8 – Variation of the environmental impacts generated during fabrication when scaling-up the membrane length. Evaluated impact categories: Climate Change (CC), Human Toxicity (HT), Acidification (AC), Freshwater Ecotoxicity (FEW), Metal Depletion (MD) and Fossil Fuel Depletion (FD).

maintained in all cases. Thus, the reproducibility of both VA-DC and ELP-PP methods to incorporate ceramic intermediate and palladium layers onto PSS tubular supports is demonstrated. Due to this similarity, a complete H₂-selectivity and almost identical permeance (deviation below 10%) to previously reported data were found. Therefore, this section has been focused on the scale-up effects on both economy and environmental impacts generated during the membrane fabrication. A similar analysis to the previously described one for the material inventory with 3 cm in length membranes is presented in Table 4 to summarize the membrane scale-up.

The study has been completed with predictions estimated for longer membrane lengths up to 100 cm, currently proposed as the maximum dimension of tubular composite membranes to be fabricated with enough guarantees. The preparation of larger membranes than 100 cm could present severe problems of homogeneity and straightness, besides the inherent complexity required in the expected production lines. Finally, a total membrane area of around 400 cm² has been maintained constant by considering different fabrication batches, independently of the particular membrane length addressed.

Fig. 7 shows the final cost per membrane area variation calculated for the fabrication of membranes progressively larger from 3 to 100 cm. As can be clearly seen, the overall membrane fabrication cost can be reduced from around 1.5 to 0.35 €/cm² by increasing the membrane length, which implies saving more than 75% of the initial estimated cost. In general, despite the need for a higher number of reactants to prepare longer membranes, they are used more efficiently. In example, a certain volume of ceramic particles suspension can be applied during VA-DC for various membrane lengths or various samples, only considering the necessity of covering the support surface completely and maintain an adequate agitation to avoid sedimentation. Something similar occurs for solutions used in the case of activation or Pd plating steps. However, it should be noted that most of these savings come from better use of electricity consumer devices in terms of available volume for each particular treatment (mainly drying or calcination). However, this trend is not linear, and the reached cost reduction decrease as the total membrane length increases. In fact, a minimum membrane fabrication cost seems to be reached for lengths in the range of 25–100 cm despite the uncertainty in the predicted data. Here it should be pointed out that further savings could be also achieved by the real industrialization of the process, although the discussed general trends surely will be maintained.

The results obtained in an analogous study for the variation of environmental impacts during the membrane scale-up reveal an almost similar trend as previously addressed for the process. Thus, the fabrication of larger composite Pd-membranes by ELP-PP onto PSS tubes with a CeO₂-based intermediate layer considerably reduces their associated negative environmental impacts in all evaluated categories. Fig. 8 collects in detail the particular environmental impacts generated in each category and refers to a concrete membrane area. The longest membrane experimentally synthesized in our laboratory (L = 250 mm) reduces the associated environmental damage by around 80% in all selected categories compared to the 30 mm membrane taken as a reference for the study. As previously discussed for the economic analysis, this fact can be

explained by the better energy efficiency of equipment, which reduces the damage associated with each membrane by increasing the membrane length. The fabrication of longer membranes up to 100 cm has also been considered to complete the study, obtaining a further reduction of the environmental footprint till 87%. These results demonstrate the viability of increasing the scale in a membrane fabrication plant from both environmental and economic point of view.

Conclusions

The current work compares both environmental and economic implications of adopting different strategies to fabricate composite membranes by Electroless Pore-Plating with diverse CeO₂-based intermediate barriers between the PSS support and the Pd-film. Particularly, the use of raw commercial dense (MB#01), porous (MB#02) or Pd-doped dense ceramic particles (MB#03) have been analyzed. The modification of raw commercial and dense particles by generating an internal porosity or doping with well-distributed fine Pd-nuclei before their deposition onto the support clearly improves the membrane performance in terms of two key parameters: Pd-thickness (being reduced from 15 to 10 or 9 μm, respectively) and H₂-permeance (increasing from 5.37 · 10⁻⁴ to 1.03 · 10⁻³ and 6.26 · 10⁻⁴ mol m⁻² s⁻¹ Pa^{-0.5}, respectively). However, both alternatives present contrary effects in environmental and economic implications. In this manner, the modification of raw and dense CeO₂ particles by doping with fine Pd nuclei before their incorporation onto the PSS support (MB#03) allows not only an improvement in the membrane performance but also the reduction of environmental damages generated during the fabrication process by an average of 27% in the selected impact categories or saving around 24% operating expenses. In this manner, the porous metal substrate becomes the most expensive part of the membrane, and future research should be run towards developing new supporting structures with adequate mechanical resistance and better morphological properties (i.e., smaller pore sizes with high porosity) but lower cost. On the contrary, the reduction of the average Pd-thickness at similar levels by using porous CeO₂ particles (MB#02) provokes adverse effects in both environmental impacts and the overall economy due to the necessity of increasing the complexity of the membrane fabrication, particularly those steps applied to modify the original morphology of PSS supports. In fact, negative environmental impacts almost double their contribution in all evaluated categories. The increase of costs during the surface modification steps by around 200% overcame the saving derived from the reached Pd-thickness reduction (–50%). Therefore, the fabrication strategy followed to prepare the membrane MB#03 has been selected as the most promising one to scale up the process at an industrial scale. In this context, it has been demonstrated that a further improvement concerning both environmental issues and economy can be reached in the fabrication of ELP-PP membranes by increasing the membrane length up to around 25 cm. However, this trend seems to stabilize for longer dimensions of tubes. All these results are essential insights to select the most adequate strategic decision about the multiple available alternatives for

fabricating Pd-based membranes. Moreover, the basis of these tools would be applied with only minor adjustments to many other membranes proposed in the specialized literature.

Declaration of Competing Interest

The authors declare that they have no known competing financial interests or personal relationships that could have appeared to influence the work reported in this paper.

Acknowledgments

The authors thank the financial support received from the Research Estate Agency (through projects with reference ENE2017-83696-R and PID2020-117273RB-I0), as well as funds coming from the Community of Madrid and Rey Juan Carlos University (through Young Researchers R&D Project Ref. M2182 - MEMRESPIP).

Abbreviations

AC	Acidification (environmental impact)
CC	Climate Change, kg CO ₂ eq (environmental impact)
ELP-PP	Electroless Pore-Plating
FD	Fossil Fuel Resources Depletion, kg oil eq (environmental impact)
FWE	Freshwater Ecotoxicity, kg 1,4-DB eq (environmental impact)
HT	Human Toxicity, kg 1,4-DB eq (environmental impact)
MD	Metal Depletion, kg Fe eq (environmental impact)
L	Membrane Length, mm or cm
LCA	Life Cycle Assessment
LCIA	Life Cycle Impact Assessment
PD	Pd-Deposition (step in membrane fabrication process)
PSS	Porous Stainless Steel
PT	Pre-Treatment (step in membrane fabrication process)
PVA	Polyvinyl alcohol (chemical)
SA	Surface Activation (step in membrane fabrication process)
SBA-15	Santa Barbara Amorphous 15 (molecular sieve)
SEM	Scanning Electron Microscopy
SM	Surface Modification (step in membrane fabrication process)
V	Volume, mL
VA-DC	Vacuum-Assisted Dip-Coating

Symbols

α_{H_2/N_2}	Ideal H ₂ /N ₂ Separation Factor
J_{H_2}	Hydrogen permeate flux, mol m ⁻² s ⁻¹
k_{H_2}	Hydrogen permeance, mol m ⁻² s ⁻¹ Pa ^{0.5}
$P_{H_2,i}$	Hydrogen Partial Pressure (in retentate -i = ret- or permeate -i = perm-), Pa

Appendix A. Supplementary data

Supplementary data to this article can be found online at <https://doi.org/10.1016/j.ijhydene.2023.04.292>.

REFERENCES

- [1] U.S. Energy Information Administration (EIA). *Monthly energy review (april)*. 2022.
- [2] Sholl DS, Lively RP. Seven chemical separation to change the world. *Nature* 2016;532:435–7.
- [3] Siddique A, Shahzad A, Lawler J, Mahmoud KA, Lee DS, Ali N, et al. Unprecedented environmental and energy impacts and challenges of COVID-19 pandemic. *Environ Res* 2020; 193:110443. <https://doi.org/10.1016/j.envres.2020.110443>.
- [4] Hosseini SE. An outlook on the global development of renewable and sustainable energy at the time of COVID-19. *Energy Res Social Sci* 2020;68:101633. <https://doi.org/10.1016/j.erss.2020.101633>.
- [5] Pal N, Agarwal M. Advances in materials process and separation mechanism of the membrane towards hydrogen separation. *Int J Hydrogen Energy* 2021;46:27062–87. <https://doi.org/10.1016/j.ijhydene.2021.05.175>.
- [6] Chen CH. Sustainable membrane technology for water and wastewater treatment. <https://doi.org/10.1007/978-981-10-5623-9>; 2017.
- [7] Baker RW. Membrane technology and applications. In: John Wiley & Sons L, editor.; 2004. p. 301–53. <https://doi.org/10.1002/0470020393.ch8>.
- [8] Zhai H. Advanced membranes and learning scale required for cost-effective post-combustion carbon capture. *iScience* 2019;13:440–51. <https://doi.org/10.1016/j.isci.2019.03.006>.
- [9] Bernardo G, Araújo T, da Silva Lopes T, Sousa J, Mendes A. Recent advances in membrane technologies for hydrogen purification. *Int J Hydrogen Energy* 2020. <https://doi.org/10.1016/j.ijhydene.2019.06.162>.
- [10] Babita K, Sridhar S, Raghavan KV. Membrane reactors for fuel cell quality hydrogen through {WGS} – review of their status, challenges and opportunities. *Int J Hydrogen Energy* 2011; 36:6671–88. <https://doi.org/10.1016/j.ijhydene.2011.02.107>.
- [11] Parvasi P, Jokar SM, Basile A, Iulianelli A. An on-board pure H₂ supply system based on a membrane reactor for a fuel cell vehicle: a theoretical study. *Membranes* 2020;10:1–17. <https://doi.org/10.3390/membranes10070159>.
- [12] Ansaloni L, Sarić M, Louradour E, Radmanesh F, Dijkstra JW, Pilz M, et al. Stability investigation of polyPOSS-imide membranes for H₂ purification and their application in the steel industry. *Int J Hydrogen Energy* 2022;47:11359–68. <https://doi.org/10.1016/j.ijhydene.2021.09.089>.
- [13] Nayeboossadri S, Speight JD, Book D. Hydrogen separation from blended natural gas and hydrogen by Pd-based membranes. *Int J Hydrogen Energy* 2019;44:29092–9. <https://doi.org/10.1016/j.ijhydene.2019.03.044>.
- [14] Dehdari L, Burgers I, Xiao P, Li KG, Singh R, Webley PA. Purification of hydrogen from natural gas/hydrogen pipeline mixtures. *Sep Purif Technol* 2022;282:120094. <https://doi.org/10.1016/j.seppur.2021.120094>.
- [15] Basile A, Jokar S, Shariati A, Iulianelli A, Rahimpour M, Dalena F, et al. Pure hydrogen production in membrane reactor with mixed reforming reaction by utilizing waste gas: a case study. *Processes* 2016;33:4. <https://doi.org/10.3390/pr4030033>.

- [16] Gao Y, Jiang J, Meng Y, Yan F, Aihemaiti A. A review of recent developments in hydrogen production via biogas dry reforming. *Energy Convers Manag* 2018;171:133–55. <https://doi.org/10.1016/j.enconman.2018.05.083>.
- [17] Sazali N, Salleh WNW, Ismail AF. Synthetic polymer-based membranes for hydrogen separation. *Synthetic polymeric membranes for advanced water treatment. Gas Separation, and Energy Sustainability* 2020:273–92. <https://doi.org/10.1016/B978-0-12-818485-1.00012-5>.
- [18] Teplyakov V. Polymeric membranes for hydrogen separation/purification. *Current Trends and Future Developments on (Bio-) Membranes* 2020:281–304. <https://doi.org/10.1016/B978-0-12-817384-8.00012-1>.
- [19] Lu GQ, da Costa JCD, Duke M, Giessler S, Socolow R, Williams RH, et al. Inorganic membranes for hydrogen production and purification: a critical review and perspective. *J Colloid Interface Sci* 2007;314:589–603. <https://doi.org/10.1016/j.jcis.2007.05.067>.
- [20] Antunes R, Böhmländer A, Bükki-Deme A, Krasch B, Cruz MM, Frances L. Experimental investigation of the ideal selectivity of MFI-ZSM-5 zeolite-type membranes for a first evaluation of the separation of hydrogen isotopologues from helium. *Sep Purif Technol* 2019;212:767–73. <https://doi.org/10.1016/J.SEPPUR.2018.11.088>.
- [21] Raso R, Tovar M, Lasobras J, Herguido J, Kumakiri I, Araki S, et al. Zeolite membranes: comparison in the separation of H₂O/H₂/CO₂ mixtures and test of a reactor for CO₂ hydrogenation to methanol. *Catal Today* 2021;364:270–5. <https://doi.org/10.1016/J.CATTOD.2020.03.014>.
- [22] Xu S, Lin X, He Y, Wang Z, Zhang Y, Liu J, et al. Carbon membrane performance on hydrogen separation in H₂H₂OHI gaseous mixture system in the sulfur-iodine thermochemical cycle. *Int J Hydrogen Energy* 2017;42:3708–15. <https://doi.org/10.1016/j.ijhydene.2016.08.101>.
- [23] Briceño K, Iulianelli A, Montané D, Garcia-Valls R, Basile A. Carbon molecular sieve membranes supported on non-modified ceramic tubes for hydrogen separation in membrane reactors. *Int J Hydrogen Energy* 2012;37:13536–44. <https://doi.org/10.1016/J.IJHYDENE.2012.06.069>.
- [24] Hashim SS, Somalu MR, Loh KS, Liu S, Zhou W, Sunarso J. Perovskite-based proton conducting membranes for hydrogen separation: a review. *Int J Hydrogen Energy* 2018;43:15281–305. <https://doi.org/10.1016/J.IJHYDENE.2018.06.045>.
- [25] Wang H, Wang X, Meng B, Tan X, Loh KS, Sunarso J, et al. Perovskite-based mixed protonic-electronic conducting membranes for hydrogen separation: recent status and advances. *J Ind Eng Chem* 2017;60:297–306. <https://doi.org/10.1016/j.jiec.2017.11.016>.
- [26] Conde JJ, Maroño M, Sánchez-Hervás JM. Pd-based membranes for hydrogen separation: review of alloying elements and their influence on membrane properties. *Separ Purif Rev* 2017;46:152–77. <https://doi.org/10.1080/15422119.2016.1212379>.
- [27] Fasolin S, Barison S, Boldrini S, Ferrario A, Romano M, Montagner F, et al. Hydrogen separation by thin vanadium-based multi-layered membranes. *Int J Hydrogen Energy* 2018;43:3235–43. <https://doi.org/10.1016/J.IJHYDENE.2017.12.148>.
- [28] Bosko ML, Dalla Fontana A, Tarditi A, Cornaglia L. Advances in hydrogen selective membranes based on palladium ternary alloys. *Int J Hydrogen Energy* 2021;46:15572–94. <https://doi.org/10.1016/J.IJHYDENE.2021.02.082>.
- [29] Jokar SM, Farokhnia A, Tavakolian M, Pejman M, Parvasi P, Javanmardi J, et al. The recent areas of applicability of palladium based membrane technologies for hydrogen production from methane and natural gas: a review. *Int J Hydrogen Energy* 2022. <https://doi.org/10.1016/J.IJHYDENE.2022.05.296>.
- [30] Alique D, Martinez-Diaz D, Sanz R, Calles JA. Review of supported pd-based membranes preparation by electroless plating for ultra-pure hydrogen production 2018;8. <https://doi.org/10.3390/membranes8010005>.
- [31] Furones L, Alique D. Interlayer properties of in-situ oxidized porous stainless steel for preparation of composite Pd membranes. *ChemEngineering* 2017;1:2. <https://doi.org/10.3390/chemengineering2010001>.
- [32] Alique D, Imperatore M, Sanz R, Calles JA, Giacinti Baschetti M, Baschetti MG. Hydrogen permeation in composite Pd-membranes prepared by conventional electroless plating and electroless pore-plating alternatives over ceramic and metallic supports. *Int J Hydrogen Energy* 2016;41:19430–8. <https://doi.org/10.1016/j.ijhydene.2016.06.128>.
- [33] Wang W, Olguin G, Hotza D, Seelro MA, Fu W, Gao Y, et al. Inorganic membranes for in-situ separation of hydrogen and enhancement of hydrogen production from thermochemical reactions. *Renew Sustain Energy Rev* 2022;160:112124. <https://doi.org/10.1016/J.RSER.2022.112124>.
- [34] Zhang K, Gao H, Rui Z, Liu P, Li Y, Lin YS. High-temperature stability of palladium membranes on porous metal supports with different intermediate layers. *Ind Eng Chem Res* 2009;48:1880–6. <https://doi.org/10.1021/ie801417w>.
- [35] Huang Y, Dittmeyer R. Preparation and characterization of composite palladium membranes on sinter-metal supports with a ceramic barrier against intermetallic diffusion. *J Membr Sci* 2006;282:296–310. <https://doi.org/10.1016/J.MEMSCI.2006.05.032>.
- [36] Martinez-Diaz D, Martínez del Monte D, García-Rojas E, Alique D, Calles JA, Sanz R. Comprehensive permeation analysis and mechanical resistance of electroless pore-plated Pd-membranes with ordered mesoporous ceria as intermediate layer. *Sep Purif Technol* 2021;258:118066. <https://doi.org/10.1016/j.seppur.2020.118066>.
- [37] Prézéus F, Tiruta-Barna L, Guigui C, Remigy JC. A generic process modelling – LCA approach for UF membrane fabrication: application to cellulose acetate membranes. *J Membr Sci* 2021:618. <https://doi.org/10.1016/j.memsci.2020.118594>.
- [38] Finkbeiner M, Inaba A, Tan RBH, Christiansen K, Klüppel HJ. The new international standards for life cycle assessment: ISO 14040 and ISO 14044. *Int J Life Cycle Assess* 2006;11:80–5. <https://doi.org/10.1065/lca2006.02.002>.
- [39] di Marcoberardino G, Binotti M, Manzolini G, Viviente JL, Arratibel A, Roses L, et al. Achievements of European projects on membrane reactor for hydrogen production. *J Clean Prod* 2017;161:1442–50. <https://doi.org/10.1016/j.jclepro.2017.05.122>.
- [40] Martinez-Diaz D, Leo P, Sanz R, Carrero A, Calles JA, Alique D. Life cycle assessment of H₂-selective Pd membranes fabricated by electroless pore-plating. *J Clean Prod* 2021; 316:128229. <https://doi.org/10.1016/j.jclepro.2021.128229>.
- [41] Maroño M, Dacuta Alessandro G, Morales A, Martinez-Diaz D, Alique D, Sánchez JM. Influence of Si and Fe/Cr oxides as intermediate layers in the fabrication of supported Pd membranes. *Sep Purif Technol* 2020;234. <https://doi.org/10.1016/j.seppur.2019.116091>.
- [42] Martinez-Diaz D, Sanz R, Calles JA, Alique D. H₂ permeation increase of electroless pore-plated Pd/PSS membranes with CeO₂ intermediate barriers. *Sep Purif Technol* 2019;216:16–24. <https://doi.org/10.1016/J.SEPPUR.2019.01.076>.
- [43] Martinez-Diaz D, Alique D, Calles JAA, Sanz R. Pd-thickness reduction in electroless pore-plated membranes by using doped-ceria as interlayer. *Int J Hydrogen Energy* 2020; 45:7278–89. <https://doi.org/10.1016/j.ijhydene.2019.10.140>.
- [44] Alique D, Sanz R, Calles JA. Pd membranes by electroless pore-plating: synthesis and permeation behavior. *Current Trends and Future Developments on (Bio-) Membranes*

- 2020:31–62. <https://doi.org/10.1016/B978-0-12-818332-8.00002-8>.
- [45] Stefanie H, Llorenç M i C. Emerging approaches, challenges and opportunities in life cycle assessment. *Science* (1979 2014;344:1109–13. <https://doi.org/10.1126/science.1248361>.
- [46] Guinée JB, Heijungs R, Huppes G, Zamagni A, Masoni P, Buonamici R, et al. Life cycle assessment: past, present, and future. *Environ Sci Technol* 2011;45:90–6. <https://doi.org/10.1021/es101316v>.
- [47] International Organization for Standardization (ISO). ISO 14040: life cycle assessment, principles and framework. 2006.
- [48] International Organization for Standardization (ISO). ISO 14044: life cycle assessment-requirements and guidelines. 2006.
- [49] Huijbregts MAJ, Steinmann ZJN, Elshout PMF, Stam G, Verones F, Vieira M, et al. ReCiPe2016: a harmonised life cycle impact assessment method at midpoint and endpoint level. *Int J Life Cycle Assess* 2017;22:138–47. <https://doi.org/10.1007/s11367-016-1246-y>.
- [50] Bare JC, Hofstetter P, Pennington DW, Udo de Haes HA. Life cycle impact assessment workshop summary. Midpoints versus endpoints: the sacrifices and benefits. *Int J Life Cycle Assess* 2000;5:319–26. <https://doi.org/10.1007/BF02978665>.
- [51] Galli F, Pirola C, Previtoli D, Manenti F, Bianchi CL. Eco design LCA of an innovative lab scale plant for the production of oxygen-enriched air. Comparison between economic and environmental assessment. *J Clean Prod* 2018;171:147–52. <https://doi.org/10.1016/j.jclepro.2017.09.268>.
- [52] Niaz F, Khan Q, Ali M, Shen W. Life-cycle assessment of ginkgo-wood three-dimensional membrane for wastewater treatment. *ACS Omega* 2020;5:4900–6. <https://doi.org/10.1021/acsomega.9b03722>.
- [53] Red Eléctrica Española. Spanish electric system. 2021. p. 2021.
- [54] Vadrucchi M, Borgognoni F, Moriani A, Santucci A, Tosti S. Hydrogen permeation through Pd–Ag membranes: surface effects and Sieverts' law. *Int J Hydrogen Energy* 2013;38:4144–52. <https://doi.org/10.1016/j.ijhydene.2013.01.091>.
- [55] Bellini S, Azzato G, Caravella A. Mass transport in hydrogen permeation through Pd-based membranes. *Current Trends and Future Developments on (Bio-) Membranes* 2020:63–90. <https://doi.org/10.1016/B978-0-12-818332-8.00003-X>.
- [56] Alique D. Processing and characterization of coating and thin film materials. In: Zhang J, Jung Y, editors. *Advanced ceramic and metallic coating and thin film materials for energy and environmental*; 2018. <https://doi.org/10.1007/978-3-319-59906-9>.